Mathematical modeling of bacterial virulence and host-pathogen interactions in the Dictyostelium/Pseudomonas system

Laura Fumanelli, Mimmo Iannelli, Hussnain Ahmed Janjua, Olivier Jousson

HAL Id: hal-00656340
https://hal.science/hal-00656340

Submitted on 4 Jan 2012

Author's Accepted Manuscript

Mathematical modeling of bacterial virulence and host-pathogen interactions in the Dictyostelium/Pseudomonas system

Laura Fumanelli, Mimmo Iannelli, Hussnain Ahmed Janjua, Olivier Jousson

www.elsevier.com/locate/yjtbi

Mathematical modeling of bacterial virulence and host-pathogen interactions in the Dictyostelium/Pseudomonas system✩

Laura Fumanelli[a,b], Mimmo Iannelli[b,*], Hussnain Ahmed Janjua[c], Olivier Jousson[c]

[a]*Fondazione Bruno Kessler (FBK), I–38123 Povo (Trento), Italy*
[b]*Department of Mathematics, University of Trento, I–38123 Povo (Trento), Italy*
[c]*Centre for Integrative Biology (CIBIO), University of Trento, I–38123 Mattarello (Trento) - Italy*

Abstract

We present some studies on the mechanisms of pathogenesis based on experimental work and on its interpretation through a mathematical model. Using a collection of clinical strains of the opportunistic human pathogen *Pseudomonas aeruginosa*, we performed co-culture experiments with *Dictyostelium* amoebae, to investigate the two organisms' interaction, characterized by a cross action between amoeba, feeding on bacteria, and bacteria exerting their pathogenic action against amoeba. In order to classify bacteria virulence, independently of this cross interaction, we have also performed killing experiments of bacteria against the nematode *C. elegans*.

A mathematical model was developed to infer how the populations of the amoeba-bacteria system evolve according to a number of parameters, taking into account the specific features underlying the interaction. The model does not fall within the class of traditional prey-predator models because not only does an amoeba feed on bacteria, but it is in turn attacked by them; thus the model must include a feedback term modeling this further interaction aspect. The model shows existence of multiple steady states and the resulting behavior of the solutions, showing bi-stability of the system, gives a qualitative explanation of the co-culture experiments.

Keywords:

Host-pathogen dynamics, Amoeba-bacteria interaction, Population models, Bi-stability

1. Introduction

Virulence is a complex and often multi-factorial phenotypic trait that quantifies the degree of pathogenicity of an organism, by establishing its ability to mount an infection and to cause a disease. Genetic determinants of bacterial virulence are potential drug targets, and represent an alternative to the generic cellular and molecular mechanisms targeted by most antibiotics used to date for the control of infections in humans and animals. Model host organisms are used to identify and study the function of virulence factors in human pathogenic bacteria. Mammalian hosts are preferentially used for this purpose, because they are thought to mimic the situation occurring in an infected human patient. However, a number of non-mammalian organisms, such as the amoeba *Dictyostelium discoideum*, the nematode *Caenorhabditis*

elegans, the insect *Drosophila melanogaster* and the fish *Danio rerio* have been recently used as alternative hosts, with the advantage of avoiding ethical problems and allowing us to assess bacterial virulence in an easier way than by using mammalian hosts.

Dictyostelium amoebae are soil microorganisms that feed on bacteria and have been utilized to assess the virulence of many different bacterial genera, including *Klebsiella* (Benghezal et al., 2006), *Aeromonas* (Froquet et al., 2007) or *Pseudomonas* (Cosson et al., 2002; Pukatzki et al., 2002). In this model system, pathogenic bacteria defend against predation by *Dictyostelium*, activating virulence pathways that impede amoeba cells to grow and to form phagocytic plaques. The system has been almost exclusively used to assess the role of specific genes in virulence, by comparing the virulence phenotype of mutants versus wild-type strains. To our knowledge, the *Dictyostelium* model has not been applied to date to determine the natural virulence range of pathogenic bacteria obtained from clinical samples.

Mathematical models concerning bacterial growth have been recently developed within different contexts motivated by nosocomial infections, though, to our knowledge, no specific model has been considered for describing the particular amoeba-bacteria interaction such as described above. In particular, some work has been devoted to modeling the interaction between pathogens and cells of the immune system (Nowak et al., 2000) or between bacteria and phagocytes, including antibiotic resistance (Austin et al., 1998; Boldin et al., 2007; D'Agata et al., 2007, 2008; Imran et al., 2007; Webb et al., 2005).

In this study, we have investigated the dynamics of virulence both per-

3

forming experimental measures and building a mathematical model for interpreting the results. We have used a collection of clinical strains of the opportunistic human pathogen *Pseudomonas aeruginosa* to perform co-culture experiments with *Dictyostelium*. The interaction between the two organisms is characterized by a cross action between amoeba, feeding on bacteria, and bacteria exerting their pathogenic action against amoeba. In order to classify bacteria virulence, independently of this cross interaction, we have also performed killing experiments of bacteria against the nematode *C. elegans*.

A mathematical model was developed to describe the growth of the amoeba-bacteria system, taking into account the specific features underlying the interaction. We discuss the behavior of the model with respect to a basic parameter representing the virulence of the bacterium. The theoretical results are compared with the experimental ones. The model does not fall within the class of traditional prey-predator models because not only does an amoeba feed on bacteria, but it is in turn attacked by bacteria that kill its cells, so that the model must include a feedback term modeling this further aspect of the interaction. The resulting model shows existence of multiple steady states and bi-stability that seems to be responsible for the observed behavior.

2. Virulence assays

The focus of this study is the investigation of the mechanisms underlying the interaction of different virulent strains of *P. aeruginosa* with *D. discoideum* NC4; nevertheless a first set of experiments with *C. elegans* N2 as a target of the pathogenic process has been performed, in order to get

4

a measure of the pathogenic action of *P. aeruginosa* independently of the predation exerted by *D. discoideum*. In fact in our context the nematode *C. elegans* N2 can be considered completely passive because during the time of the culture it does not feed on *P. aeruginosa*; thus the killing percentage that we obtain in the culture can be assumed as a measure of virulence, allowing us to order the different strains of *P. aeruginosa* according to their pathogenic strength.

2.1. Strains and growth media

A set of 27 *P. aeruginosa* clinical strains, isolated from patients suffering from urinary tract infections, wound ulcer and respiratory tract infections, were used in the experiments. *Pseudomonas aeruginosa* strains were obtained from the microbiology departments at S. Chiara Hospital of Trento (Italy) and at the University Hospital of Verona (Italy). Growth media were LB for *P. aeruginosa* culture and maintenance, SM broth for *D. discoideum* NC4 using *Klebsiella aerogenes* as a food source, and NGM agar for *C. elegans* using *E. coli* OP50 as a food source.

2.2. Virulence assays with C. elegans N2

Virulence of different strains of *P. aeruginosa* was measured independently of its interaction with *D. discoideum* by performing killing assays with *C. elegans*.

Table 1

The *C. elegans* fast killing assays (Tan et al., 1999) were performed with *P. aeruginosa* cells harvested during exponential phase, re-suspended into PG

5

broth at a final $O.D_{600}$ of 1 and spotted on PG-agar plates in a final volume of $200\mu l$ on Peptone Glucose agar plates containing sorbitol at 0.15 M. The plates were initially incubated at room temperature for 18 hours. The adult nematodes (on average 60 -70 individuals) were grown on *E. coli* OP50 on NGM plates, picked and placed on the *P. aeruginosa* spots. As a control, one plate was seeded with the non-pathogenic *E.coli* strain $DH5 - \alpha$. The plates were subsequently incubated at 22°C for 4 hours. The viability/mortality of *C. elegans* was observed under an optical microscope at 10X magnitude. Non-motile individuals were considered as dead, and the killing percentage was calculated as the ratio between dead and total *C. elegans* individuals. Clinical isolates of *P. aeruginosa* showed a wide range of virulence against *C. elegans*.

The percentage of killing ranged from 6.6% to 100% (Table 1). No mortality of *C. elegans* was observed using the non-pathogenic strain *E. coli* $DH5 - \alpha$ as a control. Among the 27 *P. aeruginosa* specimens tested, 15 were highly virulent (80-100% *C. elegans* killing), 7 strains were moderately virulent (50-80% killing) and 5 were weakly virulent or non-virulent (less than 50% killing).

2.3. Virulence assays with D. discoideum NC4

Measurements of *D. discoideum* growth on a lawn of *P. aeruginosa* were performed. Note that *D. discoideum* actually feeds only on *P. aeruginosa*.

Table 2

Pseudomonas aeruginosa cells were harvested during exponential phase, resuspended into SM broth at a final $O.D_{600}$ of 1, diluted into 5 ml of SM

6

broth and spread on SM agar plates. A total of 9 suspensions of *D. discoideum* cells in $5 - \mu$l droplets corresponding to three-fold serial dilutions of the initial culture containing 4.0×10^6 cells/ml were then spotted on lawns of each *P. aeruginosa* strain. The most concentrated droplets therefore contained about 20.000 cells, whereas the most diluted ones contained less than 10 cells. The number of *D. discoideum* cells in each dilution was controlled using an automated cell counter (Countess, Invitrogen). Serial dilutions were performed in infection medium containing HL5 and 1x Soerensen buffer mix in 1:1 ratio [50 x Soerensen buffer, K_2HPO_4 (99.86 g), Na_2HPO_4 (17.8 g), add H_2O 1000 ml]. The plates were incubated for 6 days at 19°C to visualize the growth of *D. discoideum*.

Three patterns of *Dictyostelium* growth in the presence of *P. aeruginosa* could be easily recognized: inability to form phagocytic plaques on the bacterial lawn (pattern 0, Table 2), formation of phagocytic plaques without radial dissemination of cells (pattern 1), and formation of phagocytic plaques with radial dissemination of cells leading to the formation of an annular, transparent zone around the region were *Dictyostelium* cells were spotted (pattern 2). Only the most concentrated droplets containing $2 \cdot 10^4$ or $7 \cdot 10^3$ cells were able to form phagocytic plaques on the most virulent *P. aeruginosa* isolates (growth pattern 1, Table 2), whereas the presence of a transparent annular zone (growth pattern 2) was observed only in the less virulent *P. aeruginosa* isolates, therefore confirming the reliability and coherence of results obtained from both virulence assays. *Dictyostelium* cells were also spotted on a lawn of the non-pathogenic strain *E. coli* DH5 $- \alpha$ as a control. As expected, the amoeba was able to form phagocytic plaques on DH5 $- \alpha$, even at the lowest

cell concentrations and showed the formation of the annular zone (indicating radial dissemination) when 250 cells or more were spotted.

3. A mathematical model

The experimental results reported in Table 2 possibly reveal a complex dynamics underlying the interaction between amoeba and bacteria. In fact the occurrence of survival and extinction depending on virulence and on the initial concentration of amoeba suggests the existence of different states with roles changing as virulence changes.

The process we have to model, in order to describe the interaction amoeba-bacteria, does not fall within the traditional interactions between different species because, in our case, the amoeba is at the same time a predator (since it feeds on bacteria) and a victim (since bacteria belonging to a virulent strain are able to kill amoeba cells by their pathogenic action). Having in mind this main aspect, our model is based on the following description:

- in the absence of the amoeba, bacteria follow logistic growth, with intrinsic growth rate r and carrying capacity K;

- in the absence of bacteria, the amoeboid population undergoes an exponential decay with death rate m; in fact we suppose that bacteria are their unique source of food;

- amoeba cells feed on bacteria through a mass-action like mechanism with attack rate a;

- amoeba growth occurs at a rate proportional to the uptake of bacteria, with proportionality constant d;

8

- bacteria attack and kill amoeba cells with a functional response of Holling type with handling time T and attack rate b.

All the previous statements have a precise interpretation from the modeling point of view. Denoting respectively by $u(t)$ and $v(t)$ the number of bacteria and the number of amoeba cells, our model can be written as follows:

$$
\begin{cases}
u'(t) = r\left(1 - \dfrac{u(t)}{K}\right)u(t) - au(t)v(t), \\[2mm]
v'(t) = -mv(t) + du(t)v(t) - \dfrac{bu(t)v(t)}{1 + bTv(t)}.
\end{cases}
\tag{1}
$$

By introducing the following non–dimensional variables

$$
\tilde{t} = rt \ , \ \tilde{u} = \frac{u}{K} \ , \ \tilde{v} = \frac{a}{r}v
$$

and dropping all superscripts for simplicity, system (1) becomes

$$
\begin{cases}
u'(t) = (1 - u(t))u(t) - u(t)v(t), & u(0) = u_0, \\[2mm]
v'(t) = -\mu v(t) + \delta u(t)v(t) - \gamma\dfrac{u(t)v(t)}{1 + \tau v(t)}, & v(0) = v_0,
\end{cases}
\tag{2}
$$

where

$$
\mu = \frac{m}{r} \ , \ \delta = \frac{dK}{r} \ , \ \gamma = \frac{bK}{r} \ , \ \tau = \frac{bTr}{a}
$$

and u_0 and v_0 are the initial conditions.

This rescaling has reduced the number of parameters to four and we shall discuss the model dynamics with respect to γ representing the bacterial virulence. All other parameters will be considered as fixed. In particular, since our experimental framework suggests that amoeba life-time is very large if compared with the time scale of the interactions, we will assume

$$
\mu \ll 1.
\tag{3}
$$

Moreover since we have classified virulence on the basis of killing percentage in the first four hours (see Table 1), while the amoeba growth process is measured for 6 days, we will assume

$$\tau \ll 1 \tag{4}$$

to mean that the pathogenic process is rather fast.

A first analysis to determine the dynamics of the model concerns existence of steady states.

3.1. Steady states

Here we look for steady states of system (2), namely we look for non-negative solutions of the system

$$\begin{cases} (1 - u - v)u = 0, \\ \left(-\mu + \delta u - \gamma \dfrac{u}{1 + \tau v} \right) v = 0. \end{cases} \tag{5}$$

It is immediately seen that there are always the trivial steady state $O \equiv (0,0)$ and the bacteria–only state $B \equiv (1,0)$. However, the existence of coexistence steady states, for which amoeba and bacteria densities are both strictly positive, is not so straightforward and we need to analyze the system

$$\begin{cases} 1 - u - v = 0, \\ -\mu + \delta u - \gamma \dfrac{u}{1 + \tau v} = 0, \end{cases} \tag{6}$$

or, equivalently, the intersection of the curves

$$\begin{aligned} v &= \phi_1(u) = 1 - u, \\ v &= \phi_2(u) = \frac{(\gamma - \delta)u + \mu}{\tau(\delta u - \mu)} = \frac{1}{\tau}\left(\frac{\gamma u}{\delta u - \mu} - 1 \right). \end{aligned} \tag{7}$$

10

Actually, we look for meaningful intersections of $\phi_1(u)$ and $\phi_2(u)$, i.e. such that

$$0 < u^* < 1, \quad 0 < v^* < 1. \tag{8}$$

Thus, noticing that

$$\phi_2(u) < 0 \qquad \text{for} \quad 0 < u < \frac{\mu}{\delta},$$
$$\phi_2(u) > \frac{\gamma - \delta}{\tau \delta} \quad \text{for} \quad u > \frac{\mu}{\delta},$$

we conclude that

No coexistence equilibrium exists if at least one of the following conditions is satisfied

$$\mu > \delta \tag{9}$$

$$\gamma > \delta(1 + \tau) \tag{10}$$

However we note that we can exclude case (9) because condition (3) allows to restrict to the case

$$\mu \ll \frac{\delta \tau}{1 + \tau} < \delta \tag{11}$$

and, in view of (10), we will investigate existence of equilibria against different values of the parameter $\gamma \in [0, \delta(1 + \tau)]$. To this aim we transform system (6), by substitution, into

$$\begin{cases} i) & 1 - u - v = 0, \\ ii) & \tau \delta u^2 + [\gamma - \delta(1 + \tau) - \mu\tau]\, u + \mu(1 + \tau) = 0, \end{cases} \tag{12}$$

and solve equation (12, *ii*) to get

$$u_\pm(\gamma) = \frac{[\delta(1 + \tau) - \gamma + \mu\tau] \pm \sqrt{\Delta(\gamma)}}{2\delta\tau}, \tag{13}$$

11

where

$$\Delta(\gamma) = [\delta(1+\tau) - \gamma + \mu\tau]^2 - 4\tau\delta\mu(1+\tau).$$

We have indicated dependence on γ and we actually note that the discriminant $\Delta(\gamma)$ is a decreasing function of γ, on the interval $[0, \delta(1+\tau)]$, vanishing at the point

$$\gamma^+ = \left(\sqrt{\delta(1+\tau)} - \sqrt{\mu\tau}\right)^2 < \delta(1+\tau). \tag{14}$$

Figure 1

As a consequence, (13) provides two branches $u_{\pm}(\gamma)$ of real positive solutions of (12, ii) for $\gamma \in [0, \gamma^+]$, glued at γ^+ where

$$u_-(\gamma^+) = u_+(\gamma^+) = \sqrt{\frac{\mu(1+\tau)}{\delta\tau}} < 1. \tag{15}$$

Moreover, $u_+(\gamma)$ is decreasing with γ and

$$u_+(0) = 1 + \frac{1}{\tau} > 1, \quad u_+(\gamma^*) = 1,$$

where

$$\gamma^* = \delta - \mu < \gamma^+, \tag{16}$$

so that $u_+(\gamma)$ satisfies (8) only for γ in the interval $[\gamma^*, \gamma^+]$. Concerning the other branch $u_-(\gamma)$, we have that, since

$$u_-(\gamma)u_+(\gamma) = \mu(1+\tau),$$

then $u_-(\gamma)$ is increasing and (see (15))

$$0 < u_-(\gamma) < u_-(\gamma^+) < 1.$$

12

Thus $u_-(\gamma)$ satisfies (8) for $\gamma \in [0, \gamma_+]$. Finally, taking $v_\pm(\gamma) = 1 - u_\mp(\gamma)$, we have solutions of system (12) for $\gamma \in [0, \gamma_+]$. We note (see (12)) that $v_\pm(\gamma)$ are the two solutions of

$$\delta \tau v^{*2} + [\delta - \gamma - \tau \gamma^*] v^* + \gamma - \gamma^* = 0 \qquad (17)$$

and that for $\gamma < \gamma^*$ only $v_+(\gamma)$ is positive.

In Figure 1 and Figure 2 we respectively show the bifurcation graphs of $u_\pm(\gamma)$ and $v_\pm(\gamma)$, with γ as a bifurcation parameter.

Figure 2

Next we discuss stability of the equilibria.

3.2. Stability

First of all we consider the trivial steady state $O \equiv (0,0)$ and the bacteria–only state $B \equiv (1,0)$. The respective Jacobian matrices for these states are

$$J(O) = \begin{pmatrix} 1 & 0 \\ 0 & -\mu \end{pmatrix}, \ J(B) = \begin{pmatrix} -1 & -1 \\ 0 & \gamma^* - \gamma \end{pmatrix}.$$

Consequently we have that

The trivial state O is always unstable, while B is stable if $\gamma > \gamma^*$ and unstable otherwise.

For analyzing the coexistence steady states we have to consider the Jacobian matrix

$$J(E^*) = \begin{pmatrix} -u^* & -u^* \\ \left(\delta - \dfrac{\gamma}{1+\tau v^*}\right) v^* & \dfrac{\gamma \tau u^* v^*}{(1+\tau v^*)^2} \end{pmatrix}, \qquad (18)$$

13

and analyze the sign of trace and determinant of $J(E^*)$ versus γ, along the different branches shown in Figure 2. Actually, we have

$$\text{tr} J(E^*) = \frac{u^*}{(1+\tau v^*)^2} \left(\tau^2 v^{*2} + \tau(2-\gamma)v^* + 1\right)$$

$$\det J(E^*) = \frac{u^* v^*}{(1+Tv^*)^2} \left(\delta\tau^2 v^{*2} + 2\delta\tau v^* + \delta - \gamma - \gamma\tau\right)$$

and, considering first the upper branch $v_+(\gamma) = 1 - u_-(\gamma)$, for $\gamma \in [0, \gamma^+]$, we are led to analyze the sign of

$$
\begin{aligned}
T_+(\gamma) &= \tau^2 v_+^2(\gamma) + \tau(2-\gamma)v_+(\gamma) + 1 = \\
&= \tau^2 \left(v_+(\gamma) - t_+(\gamma)\right)\left(v_+(\gamma) - t_-(\gamma)\right),
\end{aligned}
\tag{19}
$$

and

$$
\begin{aligned}
D_+(\gamma) &= \delta\tau^2 v_+^2(\gamma) + 2\delta\tau v_+(\gamma) + \delta - \gamma - \gamma\tau = \\
&= \delta\tau^2 \left(v_+(\gamma) - d_+(\gamma)\right)\left(v_+(\gamma) - d_-(\gamma)\right),
\end{aligned}
\tag{20}
$$

where

$$
\begin{aligned}
t_\pm(\gamma) &= \frac{\gamma - 2 \pm \sqrt{\gamma(\gamma-4)}}{2\tau}, \\
d_\pm(\gamma) &= \frac{-\delta \pm \sqrt{\delta\gamma(1+\tau)}}{\delta\tau},
\end{aligned}
$$

looking for positive $T_+(\gamma)$ and $D_+(\gamma)$ in order to have stability.

First we prove that

$$D_+(\gamma) \text{ is positive for } \quad \gamma \in [0, \gamma^+). \tag{21}$$

In fact, first of all, for $\gamma \leq \dfrac{\delta}{1+\tau}$, $d_\pm(\gamma)$ are both non-positive so that

$$D_+(\gamma) = \delta\tau^2 \left(v_+(\gamma) + |d_+(\gamma)|\right)\left(v_+(\gamma) + |d_-(\gamma)|\right) > 0.$$

To check the case $\gamma > \dfrac{\delta}{1+\tau}$, we note that, since $v_-(\gamma) = 1 - u_+(\gamma)$ and $v_+(\gamma) = 1 - u_-(\gamma)$ are the roots of equation (17), then the quadratic polynomial

$$P(z) = \delta\tau z^2 + \left[\delta - \gamma - \tau\gamma^*\right] z + \gamma - \gamma^*$$

14

can be written as

$$P(z) = \delta\tau \left(z - v_-(\gamma)\right)\left(z - v_+(\gamma)\right),$$

so that, for $z > 0$,

$$P(z) < 0 \quad \text{if and only if} \quad v_-(\gamma) < z < v_+(\gamma).$$

Then, after some algebra and using (14), we get

$$
\begin{aligned}
\tau\delta P\left(d_+(\gamma)\right) \\
&= 2\delta\tau(1+\tau) - (\delta + \gamma + \tau\gamma^*)\sqrt{\delta\gamma(1+\tau)} \\
&= \left[2\sqrt{\delta\gamma(1+\tau)} - \gamma - \delta(1+\tau) + \tau\mu\right]\sqrt{\delta\gamma(1+\tau)} \\
&= \left[\tau\mu - \left(\sqrt{\delta(1+\tau)} - \sqrt{\gamma}\right)^2\right]\sqrt{\delta\gamma(1+\tau)} \\
&< \left[\tau\mu - \left(\sqrt{\delta(1+\tau)} - \sqrt{\gamma^+}\right)^2\right]\sqrt{\delta\gamma(1+\tau)} = 0,
\end{aligned}
$$

so that

$$v_-(\gamma) < d_+(\gamma) < v_+(\gamma)$$

and by (20), since $d_-(\gamma) < 0$, we have (21).

Now we consider $T_+(\gamma)$ and prove

$$T_+(\gamma) \text{ is positive for } \gamma \in [0, \gamma^+). \tag{22}$$

First we note that, for $\gamma < 4$, $t_\pm(\gamma)$ are complex conjugate so that

$$4T_+(\gamma) = (2\tau v_+(\gamma) + 2 - \gamma)^2 + (4 - \gamma)\gamma > 0.$$

Thus, (22) is true if $\gamma^+ \leq 4$, while if $\gamma^+ > 4$ we are left with the case $4 \leq \gamma < \gamma^+$. To analyze this case, using

$$\tau^2 t_\pm^2(\gamma) + \tau(2 - \gamma)\, t_\pm(\gamma) + 1 = 0,$$

15

we compute

$$P\left(t_{\pm}(\gamma)\right) = \left[(\delta - 1)\gamma - \delta - \tau\gamma^*\right] t_{\pm}(\gamma) + \gamma - \gamma^* - \frac{\delta}{\tau}. \qquad (23)$$

Then, since $\tau < 1$ (see (4)) and noticing that $\gamma^+ \geq 4$ implies $\delta > 2$, we have

$$P\left(t_{\pm}(4)\right) = 2\mu + \frac{2}{\tau}(\delta - 2)(1 - \tau) > 0. \qquad (24)$$

Now, it is easy to check that, for $\gamma > 4$, the functions $t_+(\gamma)$ and $\gamma t_-(\gamma)$ are increasing with γ, while the function $t_-(\gamma)$ is decreasing. Moreover, since $\delta > 2$, $\gamma > 4$ and $\tau < 1$, we have

$$(\delta - 1)\gamma - \delta - \tau\gamma^* > (2\delta - 4) + \delta(1 - \tau) + \tau\mu > 0,$$

that, used in (23) implies that $P\left(t_{\pm}(\gamma)\right)$ is increasing and, due to (24), it is positive for $4 \leq \gamma < \gamma^+$. As a consequence, either

$$t_-(\gamma) < t_+(\gamma) < v_-(\gamma) < v_+(\gamma),$$

or

$$v_+(\gamma) < t_-(\gamma) < t_+(\gamma)$$

In both cases $T_+(\gamma) > 0$ and (22) is true.

Now we consider the lower branch of Figure 2, $v_-(\gamma) = 1 - u_+(\gamma)$, existing only for $\gamma \in [\gamma^*, \gamma^+]$.

As before we analyze the sign of

$$\begin{aligned} D_-(\gamma) &= \delta\tau^2 v_-^2(\gamma) + 2\delta\tau v_-(\gamma) + \delta - \gamma - \gamma\tau = \\ &= \delta\tau^2 \left(v_-(\gamma) - d_+(\gamma)\right)\left(v_-(\gamma) - d_-(\gamma)\right), \end{aligned} \qquad (25)$$

with

$$d_{\pm}(\gamma) = \frac{-\delta \pm \sqrt{\delta\gamma(1 + \tau)}}{\delta\tau}.$$

16

Notice that $D_-(\gamma)$ is meaningful only for $\gamma \in [\gamma^*, \gamma^+]$. We state that

$$D_-(\gamma) \ \ is \ negative \ for \quad \gamma \in [\gamma^*, \gamma^+) \tag{26}$$

(that is, the steady state associated to $v_-(\gamma)$ is always unstable). Now, proceeding as in the previous case of the upper branch, for $\gamma \leq \dfrac{\delta}{1+\tau}$, $d_\pm(\gamma)$ are both non-positive, and $D_-(\gamma)$ would be positive; but due to (11) we get that $\gamma^* \gg \dfrac{\delta}{1+\tau}$, so this is never the case.

Thus we are left with $\gamma > \dfrac{\delta}{1+\tau}$. In this case $d_-(\gamma) < 0$ and $d_+(\gamma) > 0$ and, since we have already shown that $v_-(\gamma) < d_+(\gamma) < v_+(\gamma)$, it follows that $D_-(\gamma) < 0$.

The previous results can be summarized in the following statement on the coexistence state

The coexistence state

$$(u_-(\gamma), v_+(\gamma)), \quad \gamma \in [0, \gamma^+],$$

is stable, while the state

$$(u_+(\gamma), v_-(\gamma)), \quad \gamma \in [\gamma^*, \gamma^+],$$

is unstable.

4. Comparing experiments and model behavior

The previous analysis of the model reveals that the so called bi-stable behavior, for a certain range of the parameter representing virulence, is a characteristic feature of the amoeba-bacteria interaction. A qualitative comparison of the model with the experimental results shows that the behavior is actually confirmed by data.

17

Figure 3

To discuss this point we represent the data of Tables 1 and 2 in a more significant way introducing the variable

$$m = -\ln(1 - k) \qquad (27)$$

where k is the killing percentage of a strain as determined in Table 1. m is actually proportional to the mortality induced by the pathogenic strain and is then proportional to the parameter γ introduced in the model. In Figure 3 we represent the outcome of the culture at different values of m and of the initial number v_0 of amoeba cells. Namely, we label each point (m, v_0), available from Table 2, by an index 0, 1, 2, with the following meaning

$$
\begin{aligned}
0 &= \text{amoeba extinction} , \\
1 &= \text{amoeba survival at a low density} , \qquad (28) \\
2 &= \text{amoeba survival at a high density} .
\end{aligned}
$$

This new representation can be compared with the bifurcation graph of Figure 2 and the results on stability stated in Section 3.2. In fact from this Figure 3 we see that

- for a first range of m, namely values up to $m = 2$, amoeba can survive starting with any initial number of cells; in fact, in Figure 3, all the points in the vertical strip for $m \in (0, 2)$ are labeled by 1 and 2 (but in a few isolated cases corresponding to very low values of v_0, for which we actually observe extinction); this situation corresponds to the upper branch of the bifurcation graph of Figure 2 for γ ranging in the interval

18

$[0, \gamma^*]$, where the model predicts survival for any initial v_0, since any solution is attracted by the coexistence state;

- in the interval ranging from $m = 2$ to $m = 4$, amoeba can survive only if the initial group of cells is large enough; in fact, most of the points corresponding to low values of v_0 are labeled with the index 0 and the values of v_0 necessary to gain survival is higher with higher values of m; this range corresponds to the interval $[\gamma^*, \gamma^+]$ in the graph of Figure 2, where the lower branch $v_-(\gamma)$ is unstable and works as a separatrix. In fact, low values of v_0 lead to extinction, since they belong to the basin of attraction of the state $B \equiv (1, 0)$ (corresponding to amoeba extinction), while higher values produce solutions that are attracted by the upper branch v_+ corresponding to amoeba survival;

- for values greater than $m = 4$ amoeba does not survive whatever be the initial number of cells; this situation corresponds to values of γ greater than γ^+, for which only the state $B \equiv (1, 0)$ exists and is attractive.

The correspondence described in the present work is somewhat qualitative and could be better defined if the initial and final number of amoeba cells could be counted with more accuracy. This study still provides a first insight into the mathematical laws underlying the behavior of this complex biological system made of prey-predator and host-pathogen relationships. The model and its bi-stability confirmed the importance of assessing the correct experimental parameters (mainly the initial number or concentration of amoeba cells) for an adequate application of the virulence assay for bacterial species or strains of unknown aggressiveness. Future work will focus on the

19

assessment of growth properties of bacteria and amoeba separately, including spatial patterns.
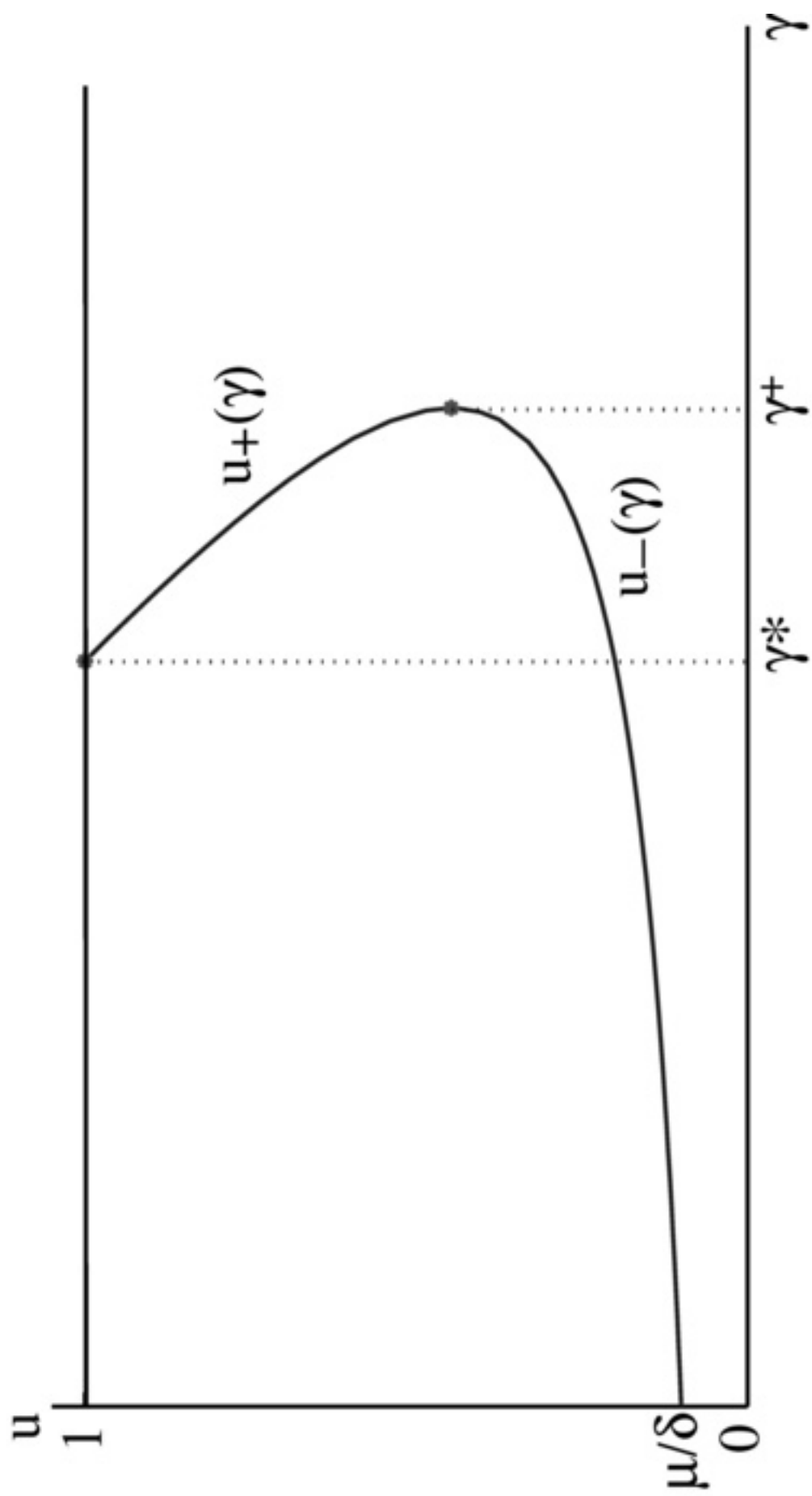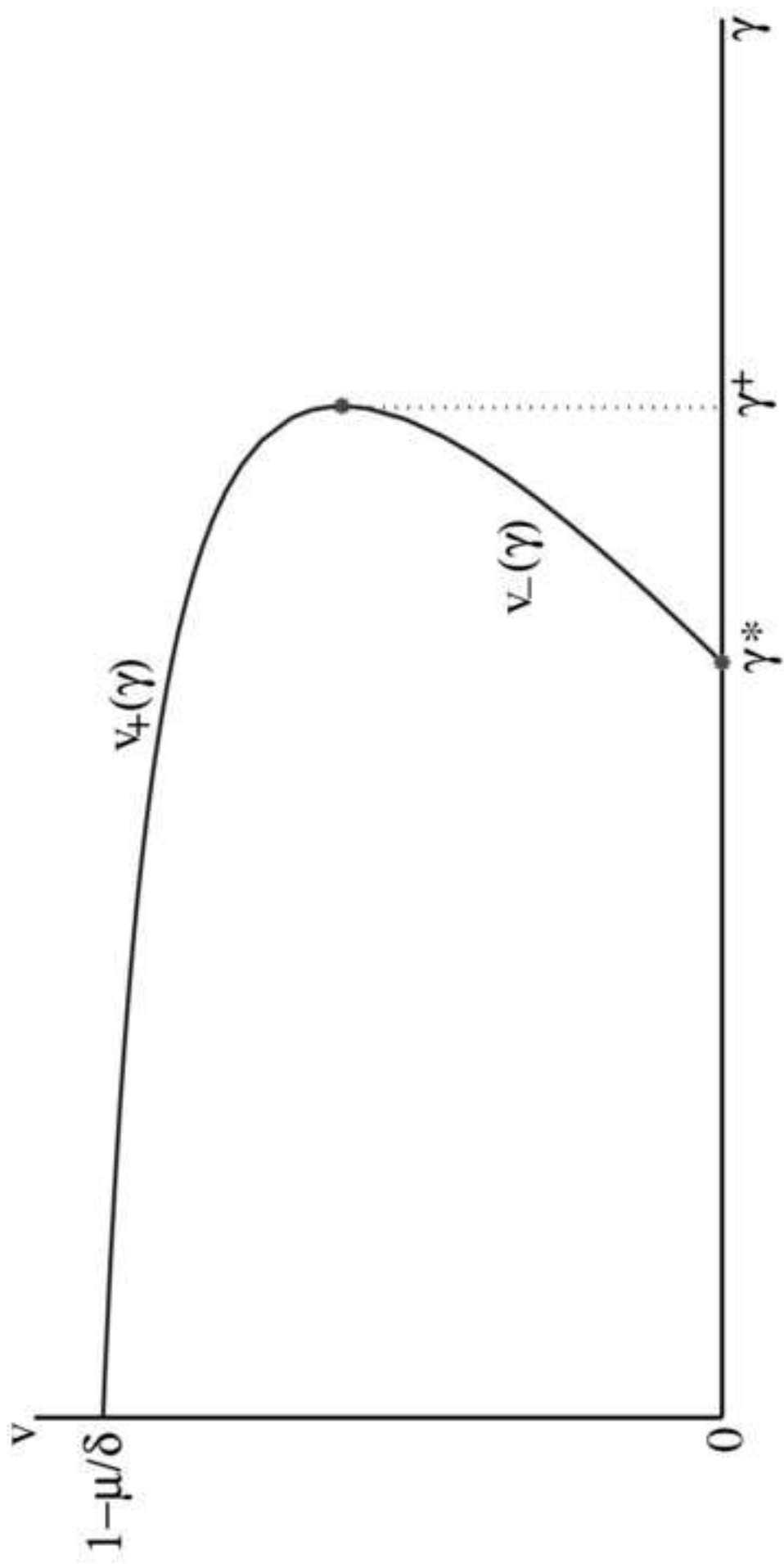
5. Acknowledgements

References

Austin, D.J., White, N.J., Anderson, R.M., 1998. The dynamics of drug action on the within-host population growth of infectious agents: melding pharmacokinetics with pathogen population dynamics. J Theor Biol 194, 313-339.

Benghezal, M., Fauvarque, M.O., Tournebize, R., Froquet, R., Marchetti, A., Bergeret, E., Lardy, B., Klein, G., Sansonetti, P., Charette, S.J., Cosson, P., 2006. Specific host genes required for the killing of Klebsiella bacteria by phagocytes. Cell Microbiol. 8 (1), 139–148.

Boldin, B., Bonten, M.J., Diekmann, O., 2007. Relative effects of barrier precautions and topical antibiotics on nosocomial bacterial transmission: Results of multi-compartment models. Bull Math Biol 69, 2227-2248.

Cosson, P., Zulianello, L., Join-Lambert, O., Faurisson, F., Gebbie, L., Benghezal, M., Van Delden, C., Curty, L.K., Khler, T., 2002. Pseudomonas aeruginosa virulence analyzed in a Dictyostelium discoideum host system. J. Bacteriol. 184 (11), 3027–3033.
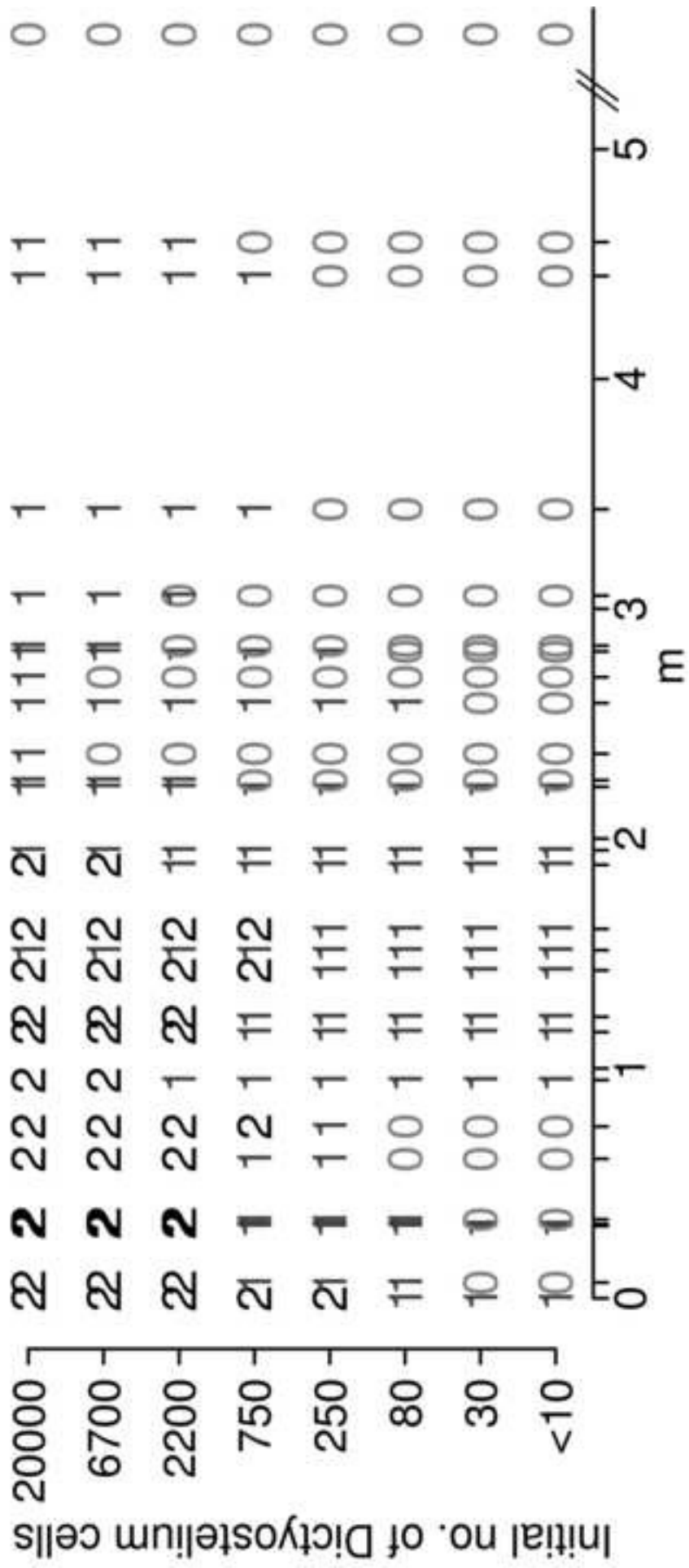
D'Agata, E.M.C., Magal, P., Olivier, D., Ruan, S., Webb, G.F., 2007. Modeling antibiotic resistance in hospitals: The impact of minimizing treatment duration. J Theor Biol 249, 487-499.

D'Agata, E.M.C., Dupont-Rouzeyrol, M., Magal, P., Olivier, D., Ruan, S., 2008. The Impact of Different Antibiotic Regimens on the Emergence of Antimicrobial-Resistant Bacteria. PLoS ONE 3, 1–9.

Froquet, R., Cherix, N., Burr, S.E., Frey, J., Vilches, S., Tomas, J.M., Cosson, P., 2007. Alternative host model to evaluate Aeromonas virulence. Appl. Environ. Microbiol. 73 (17), 5657–5659.

Imran, M., Smith, H.L., 2007. The dynamics of bacterial infection, innate immune response and antibiotic treatment. Discrete Cont Dynamical Systems B 8, 127-143.

Nowak, M.A., May, R.M., 2000. Virus dynamics. Oxford Univ. Press.

Pukatzki, S., Kessin, R.H., Mekalanos, J.J., 2002. The human pathogen Pseudomonas aeruginosa utilizes con- served virulence pathways to infect the social amoeba Dictyostelium discoideum. Proc. Natl. Acad. Sci. USA 99, 3159–3164.

Tan, M.W., Mahajan-Miklos, S., Ausubel, F.M., 1999. Killing of Caenorhabditis elegans by Pseudomonas aeruginosa used to model mammalian bacterial pathogenesis. Proc. Natl. Acad. Sci. U S A 96, 715–720.

Webb, G.F., D'Agata, E.M.C., Magal, P., Ruan, S., 2005. A model of antibiotic resistant bacterial epidemics in hospitals. Proc Natl Acad Sci USA 102, 13343-13348.

Figures Captions

- Caption for Figure 1

  Bifurcation graph concerning existence of steady states. The component $u(\gamma)$ corresponding to bacteria is represented as a function of γ. Both branches $u_+(\gamma)$ and $u_-(\gamma)$, given in (13) are shown. γ^* and γ^+ are respectively given in (16) and (14).

- Caption for Figure 2

  Bifurcation graph concerning existence of steady states. The component $v(\gamma) = 1 - u(\gamma)$ corresponding to the amoeba is represented versus γ. Both branches $v_+(\gamma) = 1 - u_-(\gamma)$ and $v_-(\gamma) = 1 - u_+(\gamma)$ are shown. γ^* and γ^+ are respectively given in (16) and (14).

- Caption for Figure 3

  Results from co-cultures of *Dictyostelium* amoebae with different strains of *Pseudomonas aeruginosa*. Different outcomes are represented according to (28) for different points (m, v_0) where m is defined in (27) and v_0 is the initial number of amoeba cells. After $m = 5$ the scale unit has been reduced.

22

4. Figure

4. Figure

4. Figure

Initial no. of Dictyostelium cells

20000
6700
2200
750
250
80
30
<10

m

0 1 2 3 4 5

strain	% killing
Hpu45	100,00
N-10	98,99
N-54	98,83
N5	96,77
N1	95,30
Hpu49	95,30
N-89	94,15
N101	94,00
N47	93,30
Hpu26	92,50
N-3	90,65
N60	89,50
N-36	89,20
N-81	85,76
Hpu75	84,84
Hpu105	79,94
Hpu47	78,00
N-85	76,00
Hpu92	70,6
N106	68,61
Hpu28A	61,30
N-30	52,64
N-11	45,47
N29	29,00
Hpu28	27,60
Hpu56	26,96
N-116	6,66
DH5-α	0,00

Table 1: *C. elegans* killing assays: different strains of *P. aeruginosa* tested agains *C. elegans*. The killing percentage is measured after 4 hours.

1

i.n.c. strain	< 10	30	80	250	750	2200	6700	20000
Hpu45	0	0	0	0	0	0	0	0
N-10	0	0	0	0	0	1	1	1
N-54	0	0	0	0	1	1	1	1
N5	0	0	0	0	1	1	1	1
N1	0	0	0	0	0	1	1	1
Hpu49	0	0	0	0	0	0	1	1
N-89	0	0	0	0	0	0	1	1
N101	0	0	0	1	1	1	1	1
N47	0	0	0	0	0	0	0	1
Hpu26	0	0	1	1	1	1	1	1
N-3	0	0	0	0	0	0	0	1
N60	0	0	0	0	0	1	1	1
N-36	1	1	1	1	1	1	1	1
N-81	1	1	1	1	1	1	1	1
Hpu75	1	1	1	1	1	1	2	2
Hpu105	1	1	1	1	2	2	2	2
Hpu47	1	1	1	1	1	1	1	1
N-85	1	1	1	1	2	2	2	2
Hpu92	1	1	1	1	1	2	2	2
N106	1	1	1	1	1	2	2	2
Hpu28A	1	1	1	1	1	1	2	2
N-30	0	0	0	1	2	2	2	2
N-11	0	0	0	1	1	2	2	2
N29	0	0	1	1	1	2	2	2
Hpu28	1	1	1	1	1	2	2	2
Hpu56	1	1	1	1	1	2	2	2
N-116	0	0	1	1	1	2	2	2
DH5	1	1	1	2	2	2	2	2

Table 1: Results of co-cultures of *D. discoideum* with different strains of *Pseudomonas aeruginosa* and different initial number of cells (i.n.c.), ranging from < 10 to 20000. Extinction of *D. discoideum* is indicated by 0, moderate growth by 1, full growth by 2.